Eur. Phys. J. C (2020) 80:1015
https://doi.org/10.1140/epjc/s10052-020-08594-4

THE EUROPEAN PHYSICAL JOURNAL C

Regular Article - Theoretical Physics

The holographic p + ip solution failed to win the competition in dRGT massive gravity

Zhang-Yu Nie[1,a], **Ya-Peng Hu**[2,b], **Hui Zeng**[1,c]

[1] Kunming University of Science and Technology, Kunming 650500, China
[2] College of Science, Nanjing University of Aeronautics and Astronautics, Nanjing 210016, China

Received: 1 May 2020 / Accepted: 21 October 2020 / Published online: 2 November 2020

Abstract In this paper, the holographic p-wave superfluid model with charged complex vector field is studied in dRGT massive gravity beyond the probe limit. The stability of p-wave and p + ip solutions are compared in the grand canonical ensemble. The p-wave solution always get lower value of grand potential than the p + ip solution, showing that the holographic system still favors an anisotropic (p-wave) solution even with considering a massive gravity theory in bulk. In the holographic superconductor models with dRGT massive gravity in bulk, a key scaling symmetry is found to be violated by fixing the reference metric parameter c_0. Therefore, in order to get the dependence of condensate and grand potential on temperature, different values of horizon radius should be considered in numerical work. With a special choice of model parameters, we further study the dependence of critical back-reaction strength on the graviton mass parameter, beyond which the superfluid phase transition become first order. We also give the dependence of critical temperature on the back reaction strength b and graviton mass parameter m^2.

1 Introduction

The AdS/CFT correspondence [1–3] provides a novel way to study the strongly coupled systems. One successful application is the so called holographic superconductor [4,5], which mimic the superconductor phase transition with a spontaneously emerged charged hair in the bulk black hole spacetime. Various different matter fields as well as gravitational theories are considered to build different holographic superconductor and superfluid models [6], in order to realize various superconducting phenomenons and to check some universal laws [7].

Superfluid with p-wave pairing has also been realized holographically. In the early study [8], an SU(2) gauge field is introduced and the three generators are used to realize the electro-magnetic vector potential and the condensed vector orders respectively, with the non-Abelian coupling between the generators act as the U(1) charged coupling. The quasi normal modes are also calculated and it turns out that the p-wave solution is stable while p + ip solution is unstable. When back reaction is turned on and becomes large enough, the p-wave phase transition becomes first order [9]. Later in Ref. [10], the p-wave phases are realized in holographic mode with five-dimensional gauged supergravities in bulk. Analytical methods are also applied to study the critical behavior of the holographic p-wave model [11]. Recent studies [12–24] reconsidered the holographic p-wave model with a charged massive vector (also called Proca field) in bulk and get more interesting phase transition phenomenon. Some efforts are made to compare the two typical p-wave models. For example, in Ref. [16], it is found that in the study of p-wave phase transitions the massive vector holographic p-wave model with $m_p^2 = 0$ repeat the same results of that in the SU(2) model. In Ref. [17], the authors compared the two p-wave models when the dark matter sector is involved in the bulk gravity theory.

Lessons on superfluid Helium-3 tell us that the superfluid phases with p-wave pairing exhibit various spatial symmetry [25]. Therefore it is interesting to study possible new phases in holographic p-wave model. Previous studies [8,26] already imply that p + ip solutions can be realized in both the two typical holographic p-wave models. However, the p + ip solution in the SU(2) p-wave model is unstable even in the probe limit. This is because the non-Abelien coupling term between the p and ip components raises the thermodynamic potential of the p + ip solution with respect to the p-wave solution. In the massive vector p-wave model, the p-wave

[a] e-mail: niezy@kust.edu.cn (corresponding author)
[b] e-mail: huyp@nuaa.edu.cn
[c] e-mail: zenghui@kust.edu.cn

and p + ip solution get the same value of grand potential and thus form a degenerate state in probe limit [26]. However, when back-reaction on the metric is turned on, the p + ip solution always get a larger value of grand potential than the p-wave solution which is more stable [26]. In order to study the properties such as conductivity and chiral magnetic effect in the p + ip phase, it would be necessary to get stable p + ip solution at first. A possible approach is extending this study in more general theories of gravity. This can also help us to understand whether the spacetime favors isotropy (p + ip solution) or anisotropy(p-wave solution) in various theories of gravity.

Recently, a ghost free gravity theory with massive graviton is proposed in Ref. [27]. The holographic dual of this massive gravity theory show translational symmetry breaking effects [28]. The holographic superconductor model with s-wave paring also has been studied in this massive gravity theory [29], giving a finite value of conductivity at zero frequency. Since the massive gravity theory has non-trivial effects in the holographic study, it would be interesting to study the problems of competition between p-wave and p + ip orders as well as the conductivity in the p + ip solution, before which building a stable p + ip solution is necessary. Some other interesting studies on dRGT massive gravity can be found in Refs. [30–37].

In this paper, we study the p-wave and p + ip solutions in a holographic model with charged complex vector field in dRGT massive gravity. We choose the massive vector model instead of the SU(2) model, because the p + ip solution in the SU(2) model is even unstable in probe limit and is more difficult to become stable when back reaction is turned on. We work in the grand canonical ensemble and compare the grand potential of the two solutions with considering the back-reaction of matter fields on metric. We also show the effect of graviton mass on this system. The rest of the paper is organized as follows. In Sect. 2 we give the set up of the new p-wave model in the massive gravity. In Sect. 3 we show the results of the stability problem between p-wave and p + ip solutions as well as the effect of graviton mass parameter. Finally, we conclude the main results in this paper and give some discussions in Sect. 4.

2 The holographic p-wave model from massive gravity

In this section, we give details of the setup of holographic p-wave model with charged complex vector field in massive gravity. We also give the expression for condensate as well as grand potential of the p-wave and p + ip solutions.

2.1 The model setup

The action can be expressed as

$$S = S_G + S_M, \tag{1}$$

$$S_G = \frac{1}{2\kappa_g^2}\int d^4x\sqrt{-g}\left(R - 2\Lambda + m^2\sum_i^4 c_i\mathcal{U}_i\right), \tag{2}$$

$$S_M = \frac{1}{q^2}\int d^4x\sqrt{-g}\left(-\frac{1}{4}F_{\mu\nu}F^{\mu\nu} - \frac{1}{2}\rho^\dagger_{\mu\nu}\rho^{\mu\nu} - m_p^2\rho^\dagger_\mu\rho^\mu\right). \tag{3}$$

The total action of this system can be divided into the gravity part and the matter part. Equation (2) is the expression for gravity part, in which the last term is the mass term for graviton. The c_i are constants and $\mathcal{U}_i$ are symmetric polynomials of the eigenvalues of the 4×4 matrix $\mathcal{K}^\mu_\nu = \sqrt{g^{\mu\alpha}f_{\alpha\nu}}$

$$\begin{aligned}
\mathcal{U}_1 &= [\mathcal{K}],\\
\mathcal{U}_2 &= [\mathcal{K}]^2 - [\mathcal{K}^2],\\
\mathcal{U}_3 &= [\mathcal{K}]^3 - 3[\mathcal{K}][\mathcal{K}^2] + 2[\mathcal{K}^3],\\
\mathcal{U}_4 &= [\mathcal{K}]^4 - 6[\mathcal{K}^2][\mathcal{K}]^2 + 8[\mathcal{K}^3][\mathcal{K}] + 3[\mathcal{K}^2]^2 - 6[\mathcal{K}^4].
\end{aligned} \tag{4}$$

The square brackets denote the trace $[\mathcal{K}] = \mathcal{K}^\mu_\mu$.

The action of the matter part (3) includes the U(1) gauge field A_μ as well as the massive complex vector field ρ_μ charged under A_μ [12,13]. The field strength of these two fields are $F_{\mu\nu} = \nabla_\mu A_\nu - \nabla_\nu A_\mu$ and $\rho_{\mu\nu} = D_\mu\rho_\nu - D_\nu\rho_\mu$ respectively, where $D_\mu = \nabla_\mu - iA_\mu$. The superscript "†" means complex conjugate, and m_p is the mass for the vector field and controls the conformal dimension of the p-wave order.

The equations of motion for this coupled system can be expressed as those for the matter fields

$$\nabla^\nu F_{\nu\mu} = i(\rho^\nu\rho^\dagger_{\nu\mu} - \rho^{\nu\dagger}\rho_{\nu\mu}), \tag{5}$$

$$D^\nu\rho_{\nu\mu} - m_p^2\rho_\mu = 0, \tag{6}$$

and the Einstein equations for the metric

$$R_{\mu\nu} - \frac{1}{2}(R - 2\Lambda)g_{\mu\nu} + m^2\mathcal{X}_{\mu\nu} = b^2\mathcal{T}_{\mu\nu}, \tag{7}$$

where $b = \kappa_g/q$ characterizes the strength of back reaction of the matter fields on the background geometry and the tensor $\mathcal{X}_{\mu\nu}$ is

$$\begin{aligned}
\mathcal{X}_{\mu\nu} = &-\frac{c_1}{2}(\mathcal{U}_1 g_{\mu\nu} - \mathcal{K}_{\mu\nu}) - \frac{c_2}{2}\left(\mathcal{U}_2 g_{\mu\nu} - 2\mathcal{U}_1\mathcal{K}_{\mu\nu} + 2\mathcal{K}^2_{\mu\nu}\right)\\
&-\frac{c_3}{2}\left(\mathcal{U}_3 g_{\mu\nu} - 3\mathcal{U}_2\mathcal{K}_{\mu\nu} + 6\mathcal{U}_1\mathcal{K}^2_{\mu\nu} - 6\mathcal{K}^3_{\mu\nu}\right)\\
&-\frac{c_4}{2}\left(\mathcal{U}_4 g_{\mu\nu} - 4\mathcal{U}_3\mathcal{K}_{\mu\nu} + 12\mathcal{U}_2\mathcal{K}^2_{\mu\nu} - 24\mathcal{U}_1\mathcal{K}^3_{\mu\nu} + 24\mathcal{K}^4_{\mu\nu}\right).
\end{aligned} \tag{8}$$

$\mathcal{T}_{\mu\nu}$ is the stress-energy tensor of the matter sector

$$\mathcal{T}_{\mu\nu} = \left(-\frac{1}{4}F^a_{\mu\nu}F^{a\mu\nu} - \frac{1}{2}\rho^\dagger_{\mu\nu|}\rho^{\mu\nu} - m_p^2\rho^\dagger_\mu\Psi^\mu\right)g_{\mu\nu} + F_{\mu\lambda}F^\lambda_\nu + \rho^\dagger_{\mu\lambda}\rho^\lambda_\nu + \rho^\dagger_{\nu\lambda}\rho^\lambda_\mu + m_p^2\left(\rho^\dagger_\mu\rho_\nu + \rho^\dagger_\nu\rho_\mu\right). \tag{9}$$

If the matter fields are turned off, the massive gravity action admits analytical solutions in the form [28]

$$\begin{aligned} ds^2 &= g_{\mu\nu}dx^\mu dx^\nu \\ &= -N(r)dt^2 + \frac{1}{N(r)}dr^2 + r^2h_{ij}dx^idx^j \\ &= -N(r)dt^2 + \frac{1}{N(r)}dr^2 + \frac{r^2}{L^2}(dx^2+dy^2), \end{aligned} \tag{10}$$

$$N(r) = c_0^2c_2m^2 + \frac{1}{2}c_0c_1m^2r - \frac{2M_0}{L^2r} + \frac{r^2}{L^2}, \tag{11}$$

while the reference metric $f_{\mu\nu}$ is taken as

$$f_{\mu\nu} = \mathrm{diag}\left(0, 0, c_0^2h_{ij}\right). \tag{12}$$

We wish to study the p-wave and vip solutions dual to superfluid phases where the U(1) symmetry is spontaneously broken. Therefore we take the ansatz for matter fields as

$$A_t = \phi(r),\ \rho_x = \Psi_x(r),\ \rho_y = i\Psi_y(r). \tag{13}$$

A metric ansatz [9,16] consistent with this matter ansatz can be given as

$$ds^2 = -N(r)\sigma(r)^2dt^2 + \frac{1}{N(r)}dr^2 + \frac{r^2}{L^2}\left(\frac{1}{f(r)^2}dx^2 + f(r)^2dy^2\right), \tag{14}$$

with

$$N(r) = c_0^2c_2m^2 + \frac{1}{2}c_0c_1m^2r - \frac{2M(r)}{L^2r} + \frac{r^2}{L^2}. \tag{15}$$

We still take the same style of reference metric $f_{\mu\nu}$ (12), where the expression for h_{ij} change to be

$$h_{ij}dx^idx^j = \frac{1}{L^2}\left(\frac{1}{f(r)^2}dx^2 + f(r)^2dy^2\right). \tag{16}$$

With the above matter and metric ansatz, we can get the full equations of motion as

$$\begin{aligned} M'(r) &= \frac{b^2L^4\phi(r)^2}{2N(r)\sigma(r)^2}\left(f(r)^2\Psi_x(r)^2 + \frac{\Psi_y(r)^2}{f(r)^2}\right) \\ &\quad + \frac{1}{2}b^2L^4N(r)\left(f(r)^2\Psi_x'(r)^2 + \frac{\Psi_y'(r)^2}{f(r)^2}\right) \\ &\quad + \frac{1}{2}b^2L^4m_p^2\left(f(r)^2\Psi_x(r)^2 + \frac{\Psi_y(r)^2}{f(r)^2}\right) \\ &\quad + \frac{b^2L^2r^2\phi'(r)^2}{4\sigma(r)^2} + \frac{L^2r^2N(r)f'(r)^2}{2f(r)^2}, \end{aligned} \tag{17}$$

$$\begin{aligned} \sigma'(r) &= \frac{b^2L^2\phi(r)^2}{rN(r)^2\sigma(r)}\left(f(r)^2\Psi_x(r)^2 + \frac{\Psi_y(r)^2}{f(r)^2}\right) \\ &\quad + \frac{b^2L^2\sigma(r)}{r}\left(f(r)^2\Psi_x'(r)^2 + \frac{\Psi_y'(r)^2}{f(r)^2}\right) \\ &\quad + \frac{r\sigma(r)f'(r)^2}{f(r)^2}, \end{aligned} \tag{18}$$

$$\begin{aligned} f''(r) &= -\frac{b^2L^2f(r)\phi(r)^2}{r^2N(r)^2\sigma(r)^2}\left(f(r)^2\Psi_x(r)^2 - \frac{\Psi_y(r)^2}{f(r)^2}\right) \\ &\quad + \frac{b^2L^2f(r)}{r^2}\left(f(r)^2\Psi_x'(r)^2 - \frac{\Psi_y'(r)^2}{f(r)^2}\right) \\ &\quad + \frac{b^2L^2m_p^2f(r)}{r^2N(r)}\left(f(r)^2\Psi_x(r)^2 - \frac{\Psi_y(r)^2}{f(r)^2}\right) \\ &\quad + \frac{f'(r)^2}{f(r)} - \frac{f'(r)N'(r)}{N(r)} - \frac{f'(r)\sigma'(r)}{\sigma(r)} - \frac{2f'(r)}{r}, \end{aligned} \tag{19}$$

$$\begin{aligned} \phi''(r) &= \left(\frac{\sigma'(r)}{\sigma(r)} - \frac{2}{r}\right)\phi'(r) \\ &\quad + \frac{2L^2}{r^2N(r)}\left(f(r)^2\Psi_x(r)^2 + \frac{\Psi_y(r)^2}{f(r)^2}\right)\phi(r), \end{aligned} \tag{20}$$

$$\begin{aligned} \Psi_x''(r) &= -\left(\frac{N'(r)}{N(r)} + \frac{\sigma'(r)}{\sigma(r)} + \frac{2f'(r)}{f(r)}\right)\Psi_x'(r) \\ &\quad - \left(\frac{\phi(r)^2}{N(r)^2\sigma(r)^2} - \frac{m_p^2}{N(r)}\right)\Psi_x(r), \end{aligned} \tag{21}$$

$$\begin{aligned} \Psi_y''(r) &= -\left(\frac{N'(r)}{N(r)} + \frac{\sigma'(r)}{\sigma(r)} - \frac{2f'(r)}{f(r)}\right)\Psi_y'(r) \\ &\quad - \left(\frac{\phi(r)^2}{N(r)^2\sigma(r)^2} - \frac{m_p^2}{N(r)}\right)\Psi_y(r). \end{aligned} \tag{22}$$

We also need to specify boundary conditions in order to solve this set of equations numerically, both on the horizon and on the $r \to \infty$ boundary of bulk AdS black brane spacetime. The boundary behaviors near horizon can be expressed as

$$M(r) = \frac{1}{2} + M_{h1}(r-r_h) + \cdots \tag{23}$$

$$\sigma(r) = \sigma_{h0} + \sigma_{h1}(r-r_h) + \cdots \tag{24}$$

$$f(r) = f_{h0} + f_{h1}(r-r_h) + \cdots \tag{25}$$

$$\phi(r) = \phi_{h1}(r-r_h) + \phi_{h2}(r-r_h)^2 + \cdots \tag{26}$$

$$\Psi_x(r) = \Psi_{xh0} + \Psi_{xh1}(r-r_h) + \cdots \tag{27}$$

$$\Psi_y(r) = \Psi_{yh0} + \Psi_{yh1}(r-r_h) + \cdots \tag{28}$$

Where the independent parameters are

$$(\sigma_{h0},\ f_{h0},\ \phi_{h1},\ \Psi_{xh0},\ \Psi_{yh0}). \tag{29}$$

The expansions near the $r \to \infty$ boundary are

$$M(r) = M_{b0} + \frac{M_{b1}}{r} + \cdots \tag{30}$$

$$\sigma(r) = \sigma_{b0} + \frac{\sigma_{b1}}{r} + \cdots \tag{31}$$

$$f(r) = f_{b0} + \frac{f_{h1}}{r} + \cdots \tag{32}$$

$$\phi(r) = \mu - \frac{\rho}{r} + \cdots \tag{33}$$

$$\Psi_x(r) = \frac{\Psi_{x-}}{r^{\Delta_-}} + \frac{\Psi_{x+}}{r^{\Delta_+}} + \cdots \tag{34}$$

$$\Psi_y(r) = \frac{\Psi_{y-}}{r^{\Delta_-}} + \frac{\Psi_{y+}}{r^{\Delta_+}} + \cdots, \tag{35}$$

where

$$\Delta_\pm = \left(1 \pm \sqrt{1 + 4m_p^2 L^2}\right)/2 \tag{36}$$

are the conformal dimensions of the source and expectation value of the dual vector operator. In this study, some constraints on the boundary coefficients ($\Psi_{x-} = 0$, $\Psi_{y-} = 0$, $\sigma_{b0} = 1$, $f_{b0} = 1$) are introduced to confirm the solutions to be asymptotically AdS and dual to a source free condensed phase.

The above knowledge tell us that with the constraints from boundary, we can get a set of solutions characterized by one parameter μ. There are also parameters including (L, b, m, m_p, c_0, c_1, c_2) which should be fixed before the numerical work.

There are several scaling symmetries in this model

1. $\Psi_x \to \lambda^2 \Psi_x$, $\Psi_y \to \lambda^2 \Psi_y$, $\phi \to \lambda^2 \phi$, $N \to \lambda^2 N$, $m_p \to \lambda m_p$, $L \to \lambda^{-1} L$, $b \to \lambda^{-1} b$, $m \to \lambda m$; (37)
2. $\Psi_x \to \lambda \Psi_x$, $\Psi_y \to \lambda \Psi_y$, $\phi \to \lambda \phi$, $N \to \lambda^2 N$, $M \to \lambda^3 M$, $r \to \lambda r$, $c_0 \to \lambda c_0$; (38)
3. $\phi \to \lambda \phi$, $\sigma \to \lambda \sigma$; (39)
4. $\Psi_x \to \lambda^{-1} \Psi_x$, $\Psi_y \to \lambda \Psi_y$, $f \to \lambda f$; (40)
5. $c_0 \to \lambda c_0$, $c_1 \to \lambda^{-1} c_1$, $c_2 \to \lambda^{-2} c_2$; (41)
6. $c_0 \to \lambda c_0$, $c_1 \to \lambda c_1$, $m \to \lambda^{-1} m$. (42)

The first four symmetries are similar to those scaling symmetries in previous study in system without graviton mass term, and the last two only involve the parameters in graviton mass term. It is the second scaling symmetry Eq. (38) that usually be used to get the varying values of temperature of the condensed solutions after solving these equations with a fixed value of horizon radius. However, in the massive gravity case this scaling symmetry involves the parameter c_0, therefore the value of c_0 changes with temperature if we use the same trick. To get solutions with the fixed value of c_0 and varying temperature, we apply a different numerical treatment in which we fix the chemical potential μ while the horizon radius r_h can be tuned to get different values of temperature with fixed value of c_0. This numerical treatment is more general than using the usual trick.

2.2 Condensates of p-wave and p + ip soluitions

With the standard shooting method and our new numerical treatment, we can get solutions dual to the ordinary p-wave states and the p + ip one respectively. In the p-wave solution we have ($\Psi_x = \Psi_p(r)$, $\Psi_y(r) = 0$(or equivalently $\Psi_x = 0$, $\Psi_y(r) = \Psi_p(r)$), and in the p + ip solution we have $\Psi_x(r) = \Psi_y(r) = \Psi_{pip}(r)$. According to the AdS/CFT dictionary, the condensed value of the orders are equal to Ψ_{x+} and Ψ_{y+} respectively. In order to better comparing the condensed value of the two different solutions, an expression of condensed value applicable for both the two solutions is [26]

$$\Psi_+ = \sqrt{\Psi_{x+}^2 + \Psi_{y+}^2}\,. \tag{43}$$

One can calculate the energy momentum tensor of the matter fields to confirm that the p-wave solution is anisotropic while the p + ip solution is isotropic (in AdS^4) [26]. In this sense, the stability relation between the two solutions also give some insights of the favor of the gravitational theory between isotropy and anisotropy.

The temperature of the boundary system is dual to the Hawking temperature of the bulk black brane

$$\begin{aligned} T &= \frac{N'(r_h)\sigma(r_h)}{4\pi} \\ &= \frac{3\sigma_{h0} r_h}{4\pi} - \frac{b^2 \phi_{h1}^2}{8\pi \sigma_{h0} r_h} + \frac{c_0 c_1 m^2 \sigma_{h0}}{4\pi} + \frac{c_0^2 c_2 m^2 \sigma_{h0}}{4\pi r_h} \\ &\quad - \frac{b^2 m_p^2 \sigma_{h0}}{4\pi r_h}\left(f_{h0}^2 \Psi_{xh0}^2 + \frac{\Psi_{yh0}^2}{f_{h0}^2}\right). \end{aligned} \tag{44}$$

As we have explained in the previous section, the second scaling symmetry Eq. (38) involve the parameter c_0 and we can not easily get the condensed solutions with varying temperature by using the scaling trick. In order to solve this problem, we explore new numerical technic to get solutions with a varying horizon radius r_h and fixed value of chemical potential $\mu = 3$.

We can draw condensed value of the both solution with respect to temperature T once we fixed a set of values (L, b, m, m_p, c_0, c_1, c_2) and solved the equations of motion numerically. In this work we focus on the effect of graviton mass, we set $L = 1$ and $c_0 = c_1 = -2c_2 = 1$ for simplicity [29–31]. With such a choice of parameters, the numerical work involving the metric tensor will be simplified a lot.

If we take probe limit $b \to 0$, because the symmetry between the equations of motion for Ψ_x and Ψ_y, the p-wave and p + ip solutions will have the same value of critical temperature, condensate as well as grand potential [26]. If we go

beyond the probe limit with finite value of b, the degenerate p-wave and p + ip solutions will still have the same values of critical temperature, but the condensate and grand potential curves of the two solutions will be split gradually away from the critical point. In Einstein gravity, the p-wave solution always have a lower grand potential, the p + ip solution only could be stable when the p-wave solution does not exist in that region.

2.3 Grand potential of p-wave and p + ip soluitions

We wish to study the stability problem between the p wave and p + ip solutions in this massive gravity setup, and it is necessary to calculate the grand potential of this system. We work in the grand canonical ensemble and the grand potential is given by the Euclidean on-shell action.

$$\Omega = T S_E. \tag{45}$$

Besides the bulk action (1), a Gibbons–Hawking term

$$S_{GH} = -\frac{1}{\kappa_g^2}\int_\Sigma d^3x\sqrt{-\gamma}K\ . \tag{46}$$

as well as a counter term

$$S_{ct} = -\frac{1}{\kappa_g^2}\int_\Sigma d^3x\sqrt{-\gamma}\left(\frac{2}{L}+\frac{1}{2}R[\gamma] +\frac{1}{4}m^2L\left(c_1\mathcal{U}_1-\frac{1}{16}L^2m^2c_1^2\mathcal{U}_1^2+2c_2\mathcal{U}_2\right)\right), \tag{47}$$

where Σ denotes the boundary hyper surface at $r\to\infty$ and $R[\gamma]$ is the Ricci scalar of the induced metric $\gamma_{\mu\nu}$ on Σ, should also be included [38]. Therefore

$$S_E = \left(S + S_{GH} + S_{ct}\right)_{Euclidean}\ . \tag{48}$$

With our metric and matter ansatz (13, 14), the expression for the grand potential density Ω is

$$\begin{aligned}\kappa_g^2V_2\Omega = &\int_{r_h}^\infty\left(\frac{c_0^2c_2m^2\sigma(r)}{L^2}+\frac{c_0c_1m^2r\sigma(r)}{2L^2}\right)dr\\ &-\frac{rN(r)\sigma(r)}{L^2}\Big|_{r=\infty}\\ &+\sqrt{N(r)}\frac{\left(r^2\sqrt{N(r)}\sigma(r)\right)'}{L^2}\Big|_{r=\infty}\\ &+\sqrt{N(r)}\sigma(r)\left(\frac{c_0c_1m^2r-2c_0^2c_2m^2}{2L}\right.\\ &\left.+\frac{c_0^2c_1^2m^4L}{16}-\frac{2r^2}{L^3}\right)\Big|_{r=\infty},\end{aligned} \tag{49}$$

where $V_2=\int dxdy$ is the volume of the boundary system.

The terms in the first line are the contribution from bulk action, the term in the second line is from the Gibbons-Hawking term and the last line show the contribution from boundary counter terms. Both the bulk integration term and the boundary terms are divergent, but the sum of the two is convergent. We take the boundary term into the integration to get a convergent result in our numerical work

$$\begin{aligned}\kappa_g^2V_2\Omega = &\int_{r_h}^\infty\left(\frac{c_0^2c_2m^2\sigma(r)}{L^2}+\frac{c_0c_1m^2r\sigma(r)}{2L^2}\right)dr\\ &+\int_{r_h}^\infty\left[-\frac{rN(r)\sigma(r)}{L^2}\right.\\ &+\sqrt{N(r)}\frac{\left(r^2\sqrt{N(r)}\sigma(r)\right)'}{L^2}\\ &+\sqrt{N(r)}\sigma(r)\left(\frac{c_0c_1m^2r-2c_0^2c_2m^2}{2L}\right.\\ &\left.\left.+\frac{c_0^2c_1^2m^4L}{16}-\frac{2r^2}{L^3}\right)\right]'dr\\ &+\left[-\frac{rN(r)\sigma(r)}{L^2}+\sqrt{N(r)}\frac{\left(r^2\sqrt{N(r)}\sigma(r)\right)'}{L^2}\right.\\ &+\sqrt{N(r)}\sigma(r)\left(\frac{c_0c_1m^2r-2c_0^2c_2m^2}{2L}\right.\\ &\left.\left.+\frac{c_0^2c_1^2m^4L}{16}-\frac{2r^2}{L^3}\right)\right]\Big|_{r=r_h}.\end{aligned} \tag{50}$$

The final expression is

$$\begin{aligned}\kappa_g^2V_2\Omega = &\int_{r_h}^\infty\left(\frac{N(r)\sigma(r)}{L^2}-\frac{4r\sqrt{N(r)}\sigma(r)}{L^3}+\frac{2r\sigma(r)N'(r)}{L^2}\right.\\ &+\frac{3rN(r)\sigma'(r)}{L^2}+\frac{r^2\sigma(r)N'(r)}{L^3\sqrt{N(r)}}+\frac{2r^2\sqrt{N(r)}\sigma'(r)}{L^3}\\ &+\frac{2r^2N'(r)\sigma'(r)}{2L^2}+\frac{r^2\sigma(r)N''(r)}{2L^2}+\frac{r^2N(r)\sigma''(r)}{L^2}\\ &\frac{c_0^2c_2m^2\sigma(r)}{L^2}+\frac{c_0c_1m^2r\sigma(r)}{2L^2}\\ &-\frac{c_0c_1m^2\sqrt{N(r)}\sigma(r)}{2L}-\frac{c_0c_1m^2r\sqrt{N(r)}\sigma'(r)}{2L}\\ &-\frac{c_0c_1m^2r\sigma(r)N'(r)}{4L\sqrt{N(r)}}-\frac{c_0^2c_2m^2\sqrt{N(r)}\sigma'(r)}{L}\\ &-\frac{c_0^2c_2m^2\sigma(r)N'(r)}{2L\sqrt{N(r)}}+\frac{c_0^2c_1^2m^2L\sqrt{N(r)}\sigma'(r)}{16}\\ &\left.+\frac{c_0^2c_1^2m^2L\sigma(r)N'(r)}{32\sqrt{N(r)}}\right)dr+\frac{r^2\sigma(r)N'(r)}{2L^2}\Big|_{r=r_h}.\end{aligned} \tag{51}$$

With the above formulas in hand, we studied the competition between the p-wave and p + ip solutions as well as the phase structure of this holographic system. We show our main results in the next section.

3 Competition between the two solutions and the influence of m^2 on T_c

We get the two solutions numerically and compared the grand potential of the two. Unfortunately, the p + ip solution still failed to win the competition with the choice of parameters we considered. The figures of temperature dependence of condensate value as well as grand potential are qualitatively the same to the results in Einstein gravity [26]. Therefore we only show a typical case, in which the p-wave solution is a first order phase transition while the p + ip one is still second order, with $m^2 = 0.3$ and $b = 0.68$ in Fig. 1.

We can see from Fig. 1 that the p-wave and p + ip solutions share the same critical point, which can be explained by the degeneration of the two solutions in probe limit [26]. The p-wave solution with a first order phase transition has a larger value of phase transition temperature. We can also see from the right plot of free energy curves that the one with a first order phase transition get lower value of free energy than the one with second order phase transition.

Although we failed to find stable p + ip solutions, we still wish to find some qualitative estimation of the stability relation between the two solutions. One useful signal of stability can be taken as the critical back reaction strength b_c, beyond which the phase transition is first order. From the condensate and grand potential curves in Fig. 1 and in Ref. [26], we can see that the phase transition of the more stable p-wave solution change from second order to first order at a lower critical value of back reaction strength. We denote this critical value of back reaction strength for the p-wave and p + ip solutions as b_{c-p} and b_{c-pip} respectively. Between the two solutions sharing the same critical point, the more stable one always get a lower value of b_c. Therefore the stability relation of the two solutions can be concretely shown from the value of b_{c-p} and b_{c-pip}.

In this paper, we focus on the influence of m^2 on the stability relation of the two solutions as well as phase structure. We show these results in the following sections.

3.1 b_{c-p} v.s. b_{c-pip}

In this section, we give the dependence of b_{c-p} and b_{c-pip} on the value of m^2. This will show a qualitative stability relation between the two solutions, and help to confirm that the p-wave solution is always more stable.

We have set $\mu = 3$ and $L = 1, c_0 = c_1 = -2c_2 = 1$, and consider two typical values 0 and $-3/16$ for m_p^2 as in Refs. [12,26]. The massive vector p-wave model with $m_p^2 = 0$ can repeat the same p-wave phase transition as the SU(2) p-wave model [16], while with $m_p^2 = -3/16$, a typical zeroth order phase transition occur in the low temperature region [12]. As we choose the same values of m_p^2 as in Ref. [26], it is convenient to compare our results in massive gravity with previous study in Einstein gravity. To show the influence of graviton mass on the stability relation, we varying the value of the graviton mass parameter m^2 and draw the two curves of b_{c-p} and b_{c-pip} in Fig. 2, where the left plot show the case of $m_p^2 = 0$ and the right plot show the one with $m_p^2 = -3/16$. The solid blue line denote the $b_c - m^2$ relation for the p-wave solution and the dashed red line denote the relation for p + ip solution. The points on each line indicate the location of the minimum.

At the beginning, we only consider positive values of m^2. We can see that in both the two cases ($m_p^2 = 0$ and $m_p^2 = -3/16$), the value of b_c for the two solutions all increase monotonically when the value of m^2 is increasing. To study the trend of the stability relation of the two solutions, we further draw the ratio b_{c-pip}/b_{c-p} versus m^2 curves in Fig. 3. The solid orange line is for the case with $m_p^2 = 0$ and the dashed purple line for the case with $m_p^2 = -3/16$, with the two points on each line indicating the minimum.

We can see that for positive values of m^2, the ratio b_{c-pip}/b_{c-p} is larger than 1 and is monotonically increasing function of m^2. Therefore if we further decrease the value of m^2 to some negative value, it is possible that b_{c-pip}/b_{c-p} becomes less than 1, which is a signal of a stable p + ip solution. In order to exclude this possibility, we extend our results to include negative values of m^2 and complete the left part of the curves in Figs. 2 and 3. We can see that for both the two cases ($m_p^2 = 0$ and $m_p^2 - 3/16$), b_{c-p}, b_{c-pip} and the ratio b_{c-pip}/b_{c-p} all get a minimum at some negative value of m^2. Especially, the minimum of the ratio b_{c-pip}/b_{c-p} is still larger than 1, indicating that it is not likely to make the p + ip solution win the competition against the p-wave one by tuning m^2.

The validity of negative value of m^2 can be understood from the following two aspects. On one side, the mass of the fields in AdS can get negative value above the B-F bound, such a bound may also be available for the graviton mass. On the other side, the minus sign of m^2 can be equivalently moved to the parameters c_1 and c_2. Thus the same results can be get from effectively considering positive value of m^2 and $c_1 = -2c_2 = -1$.

3.2 Critical temperature

Because the p-wave solution always win the competition, the phase structure of this system is rather simple. It only include the normal phase in high temperature region and the p-wave phase in low temperature region. Another feature is that the phase transition becomes first order when the back reaction is strong enough. When the phase transition becomes first order, the phase transition point get a higher temperature than the

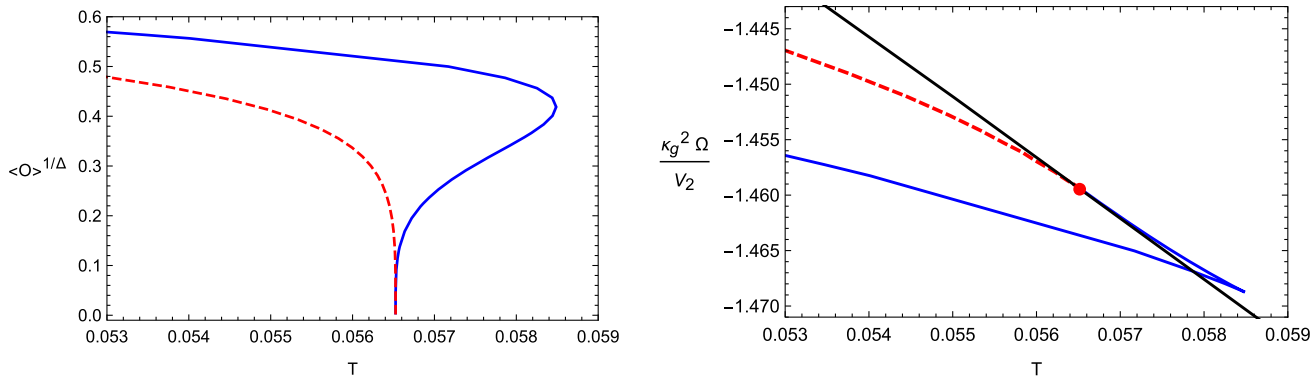

Fig. 1 Then condensate (left plot) and grand potential (right plot) curves for the p-wave and p + ip solutions with $m^2 = 0.3$ and $b = 0.68$. We use solid blue line to denote the curves for p-wave solution and the dashed red line for the p + ip solution. The solid black line denote the grand potential curve for the normal solution without any condensate

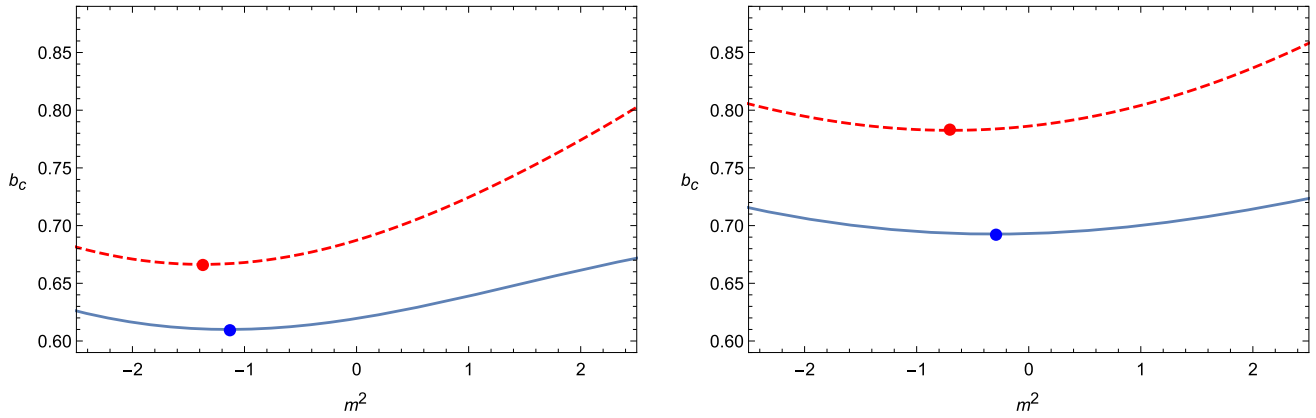

Fig. 2 $b_c - m^2$ relations for $m_p^2 = 0$ (left plot) and $m_p^2 = -3/16$ (right plot). The solid blue line denote the $b_c - m^2$ relation for the p-wave solution and the dashed red line denote the relation for p + ip solution, with the points on each line indicating the location of the minimum

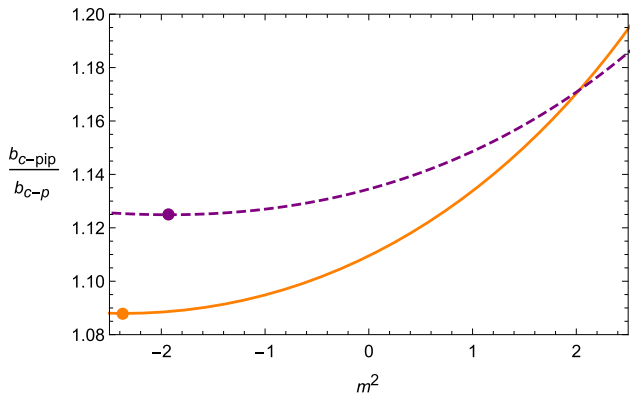

Fig. 3 $b_{c-pip}/b_{c-p} - m^2$ relations. The solid orange line is for the case with $m_p^2 = 0$ and the dashed purple line for the case with $m_p^2 = -3/16$, with the two points on each line indicating the minimum

"critical point" where the condensate emerge from the norm phase.

We studied the impact of graviton mass parameter m^2 on the critical temperature of p-wave condensate only for $m_p^2 = 0$, because the other case $m_p^2 = -3/16$ involve 0th order phase transitions at lower temperature, which make it complicated to get the phase diagram and is not the focus of this work. Because the back reaction strength also affect the critical temperature, we start from the probe limit $b = 0$ and draw the relation of $m^2 - T_c$ in the left plot of Fig. 4. This plot is also a 2D phase diagram in probe limit.

We can see from this plot that the critical temperature get a maximum at a positive value of $m^2 = 1.30$. To under stand this non-monotonic behavior, we can see the formula Eq. (44) for temperature. In probe limit, only the first term proportional to r_h and two terms proportional to m^2 left in that formula. We confirmed that when m^2 is increasing, the value of r_h and the first term in Eq. (44) for the critical point decrease monotonically. However, the increasing of m^2 has an effect of increasing the critical temperature through the two terms in Eq. (44). As a result, the final dependence of T_c on m^2 show a non-monotonic behavior combining the above two effects.

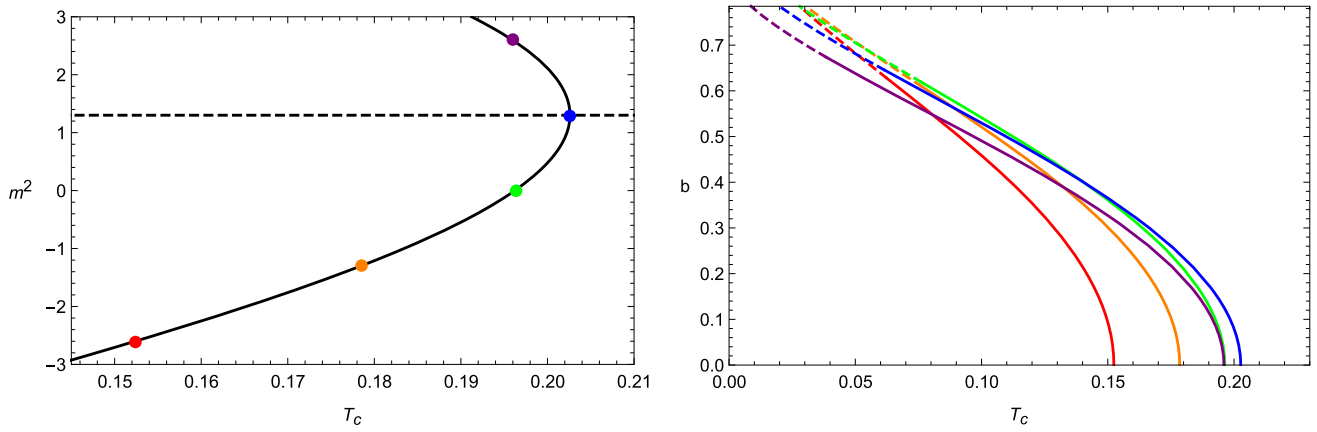

Fig. 4 $m^2 - T_c$ relation at probe limit (left plot) and $b - T_c$ relations (right plot) in the case $m_p^2 = 0$. In the left plot, we show the $T_c - m^2$ relation of the p-wave phase when back reaction can be neglected, while in the right plot we show the $b - T_c$ curves for the critical points with five values of m^2. The dashed black horizontal line in the left figure indicate the maximum critical temperature at $m^2 = 1.30$. In both the two plots, the five colors {red, orange, green, blue, purple} are used to denote five values of m^2: {-2.6, -1.3, 0.01, 1.3, 2.6}

To get more information away from the probe limit, we choose five values of m^2 and show the $b - T_c$ curves in the right plot of Fig. 4. We use {Red, Orange, Green, Blue, Purple} to denote the lines with $m^2 = \{-2.6, -1.3, 0.01, 1.3, 2.6\}$ respectively. We also mark the five points with the selected value of m^2 in the left plot with the same color assignment. In the right plot of Fig. 4, the solid lines are all real boundary of the p-wave phase, therefore the five solid lines also describe 2D slices of the phase diagram at different values of m^2. The dashed lines denote the "critical point" of the first order phase transition, and has a temperature lower than the real phase transition point.

Because of the non-monotonic effect of m^2, the relation of the five colored lines are complicated. In general, we can see that all these lines show a decreasing of critical temperature when the back reaction strength is increasing. The one with a larger value of m^2 has more decreasing of critical temperature, which can be attributed to the last two terms in Eq. (44).

4 Conclusions and discussions

In this paper, we studied the complex vector p-wave mode within dRGT massive gravity. We considered the full back reaction and study the competition between the p-wave and p + ip solutions, and find that the p-wave solution still always win the competition. We also compare the value of critical back reaction strength, beyond which the phase transition become first order, to show a qualitative stability relation. We also give the value of critical temperature at different values of graviton mass parameter m^2 and back reaction strength b.

In the case of dRGT massive gravity, a key scaling symmetry involve the parameter c_0, therefore one can not use the scaling trick to easily get dependence of temperature with a fixed value of c_0. To solve this problem, we take varying value of r_h in our numerical work to get the varying temperature directly, which is a more general numerical treatment.

Since the p + ip solution still failed to win the competition against the p-wave one, we can continue exploring this competition in new setups. With in this study, we find that the ratio b_{c-pip}/b_{c-p} can be a convenient signal to be used in future study.

When we finished the draft of this work, a similar subject was treated in Ref. [39], which focus on the analytical study of the p-wave superconductor phase transition in massive gravity in probe limit. The authors get the analytical expressions for the critical temperature, condensate of the p-wave order as well as the difference of free energy between normal solution and the p-wave solution. They also show the influence of the massive gravity parameters on the above quantities. Compared to that work, we go beyond probe limit and studied the competition between the p-wave and p + ip solutions with numerical method, while focusing on the case $c_0 = c_1 = -2c_2 = 1$.

Acknowledgements ZYN would like to thank Qi-Yuan Pan for useful discussions and suggestions. This work was supported in part by the National Natural Science Foundation of China under Grant Nos. 11565017, 11965013, and 11575083. ZYN is supported in part by Yunnan Ten Thousand Talents Plan Young & Elite Talents Project.

Data Availability Statement This manuscript has no associated data or the data will not be deposited. [Authors' comment: Our study involves some numerical calculations, which can be easily repeated with the formulas in this paper.]

Funded by SCOAP[3].

References

1. J.M. Maldacena, The large N limit of superconformal field theories and supergravity. Adv. Theor. Math. Phys. **2**, 231 (1998). arXiv:hep-th/9711200 [**Int. J. Theor. Phys. 38, 1113 (1999)**]
2. S.S. Gubser, I.R. Klebanov, A.M. Polyakov, Gauge theory correlators from non-critical string theory. Phys. Lett. B **428**, 105 (1998). arXiv:hep-th/9802109
3. E. Witten, Anti-de Sitter space and holography. Adv. Theor. Math. Phys. **2**, 253 (1998). arXiv:hep-th/9802150
4. S.S. Gubser, Breaking an Abelian gauge symmetry near a black hole horizon. Phys. Rev. D **78**, 065034 (2008). arXiv:0801.2977 [hep-th]
5. S.A. Hartnoll, C.P. Herzog, G.T. Horowitz, Building a holographic superconductor. Phys. Rev. Lett. **101**, 031601 (2008). arXiv:0803.3295 [hep-th]
6. R.G. Cai, L. Li, L.F. Li, R.Q. Yang, Introduction to holographic superconductor models. Sci. China Phys. Mech. Astron. **58**(6), 060401 (2015). arXiv:1502.00437 [hep-th]
7. J. Zaanen, Y.W. Sun, Y. Liu, K. Schalm, *Holographic duality in condensed matter physics* (Cambridge University Press, Cambridge, 2015)
8. S.S. Gubser, S.S. Pufu, The gravity dual of a p-wave superconductor. JHEP **0811**, 033 (2008). arXiv:0805.2960 [hep-th]
9. M. Ammon, J. Erdmenger, V. Grass, P. Kerner, A. O'Bannon, On holographic p-wave superfluids with Back-reaction. Phys. Lett. B **686**, 192 (2010). arXiv:0912.3515 [hep-th]
10. F. Aprile, D. Rodriguez-Gomez, J.G. Russo, p-wave holographic superconductors and five-dimensional gauged supergravity. JHEP **01**, 056 (2011). arXiv:1011.2172 [hep-th]
11. S. Gangopadhyay, D. Roychowdhury, Analytic study of properties of holographic p-wave superconductors. JHEP **08**, 104 (2012). arXiv:1207.5605 [hep-th]
12. R.G. Cai, L. Li, L.F. Li, A holographic P-wave superconductor model. JHEP **1401**, 032 (2014). arXiv:1309.4877 [hep-th]
13. R.G. Cai, S. He, L. Li, L.F. Li, A holographic study on vector condensate induced by a magnetic field. JHEP **1312**, 036 (2013). arXiv:1309.2098 [hep-th]
14. L.F. Li, R.G. Cai, L. Li, C. Shen, Entanglement entropy in a holographic p-wave superconductor model. Nucl. Phys. B **894**, 15 (2015). arXiv:1310.6239 [hep-th]
15. Y.B. Wu, J.W. Lu, W.X. Zhang, C.Y. Zhang, J.B. Lu, F. Yu, Holographic p-wave superfluid. Phys. Rev. D **90**(12), 126006 (2014). arXiv:1410.5243 [hep-th]
16. Z.Y. Nie, R.G. Cai, X. Gao, L. Li, H. Zeng, Phase transitions in a holographic s + p model with back-reaction. Eur. Phys. J. C **75**, 559 (2015). arXiv:1501.00004 [hep-th]
17. M. Rogatko, K.I. Wysokinski, P-wave holographic superconductor/insulator phase transitions affected by dark matter sector. JHEP **03**, 215 (2016). arXiv:1508.02869 [hep-th]
18. Q. Pan, S.J. Zhang, Revisiting holographic superconductors with hyperscaling violation. Eur. Phys. J. C **76**(3), 126 (2016). arXiv:1510.09199 [hep-th]
19. C. Lai, Q. Pan, J. Jing, Y. Wang, Analytical study on holographic superfluid in AdS soliton background. Phys. Lett. B **757**, 65 (2016). arXiv:1601.00134 [hep-th]
20. R. Arias, I. Salazar Landea, Spontaneous current in an holographic s+p superfluid. Phys. Rev. D **94**(12), 126012 (2016). arXiv:1608.01687 [hep-th]
21. J.W. Lu, Y.B. Wu, B.P. Dong, H. Liao, Holographic p-wave superconductor in Lifshitz gravity with RF^2 correction. Phys. Lett. B **785**, 517 (2018)
22. J.W. Lu, Y.B. Wu, B.P. Dong, Y. Zhang, Holographic p-wave superconductor with C^2F^2 correction. Eur. Phys. J. C **80**(2), 114 (2020)
23. Y. Huang, Q. Pan, W.L. Qian, J. Jing, S. Wang, Holographic p-wave superfluid with Weyl corrections. Sci. China Phys. Mech. Astron. **63**(3), 230411 (2020)
24. Y. Lv, X. Qiao, M. Wang, Q. Pan, W.L. Qian, J. Jing, Holographic p-wave superfluid in the AdS soliton background with RF 2 corrections. Phys. Lett. B **802**, 135216 (2020). arXiv:2001.08364 [hep-th]
25. D. Vollhardt, P. Wolfle, *The superfluid phases of helium 3* (Taylor and Francis Inc., Philadelphia, 1990)
26. Z.Y. Nie, Q. Pan, H.B. Zeng, H. Zeng, Split degenerate states and stable p $+i$ p phases from holography. Eur. Phys. J. C **77**(2), 69 (2017). arXiv:1611.07278 [hep-th]
27. C. de Rham, G. Gabadadze, A.J. Tolley, Resummation of massive gravity. Phys. Rev. Lett. **106**, 231101 (2011). arXiv:1011.1232 [hep-th]
28. D. Vegh, Holography without translational symmetry (2013). arXiv:1301.0537 [hep-th]
29. H.B. Zeng, J.P. Wu, Holographic superconductors from the massive gravity. Phys. Rev. D **90**(4), 046001 (2014). arXiv:1404.5321 [hep-th]
30. Y.P. Hu, H.F. Li, H.B. Zeng, H.Q. Zhang, Holographic Josephson junction from massive gravity. Phys. Rev. D **93**(10), 104009 (2016). arXiv:1512.07035 [hep-th]
31. Y.P. Hu, X.X. Zeng, H.Q. Zhang, Holographic thermalization and generalized Vaidya-AdS solutions in massive gravity. Phys. Lett. B **765**, 120 (2017). arXiv:1611.00677 [hep-th]
32. R.G. Cai, Y.P. Hu, Q.Y. Pan, Y.L. Zhang, Thermodynamics of black holes in massive gravity. Phys. Rev. D **91**(2), 024032 (2015). arXiv:1409.2369 [hep-th]
33. Y.P. Hu, H. Zhang, Misner-sharp mass and the unified first law in massive gravity. Phys. Rev. D **92**(2), 024006 (2015). arXiv:1502.00069 [hep-th]
34. J. Xu, L.M. Cao, Y.P. Hu, P–V criticality in the extended phase space of black holes in massive gravity. Phys. Rev. D **91**(12), 124033 (2015). arXiv:1506.03578 [gr-qc]
35. Y.P. Hu, F. Pan, X.M. Wu, The effects of massive graviton on the equilibrium between the black hole and radiation gas in an isolated box. Phys. Lett. B **772**, 553 (2017). arXiv:1703.08599 [gr-qc]
36. B. Eslam Panah, S. Hendi, Y. Ong, Black hole remnant in massive gravity. Phys. Dark Univ. **27**, 100452 (2020). arXiv:1808.07829 [gr-qc]
37. B.Eslam Panah, S. Hendi, Black hole solutions correspondence between conformal and massive theories of gravity. EPL **125**(6), 60006 (2019). arXiv:1904.07670 [gr-qc]
38. L.M. Cao, Y. Peng, Counterterms in massive gravity theory. Phys. Rev. D **92**(12), 124052 (2015). arXiv:1509.08738 [hep-th]
39. C.H. Nam, Effects of massive gravity on p-wave holographic superconductor. Phys. Lett. B **807**, 135547 (2020). arXiv:2004.00861 [hep-th]